Kinetics of spinodal phase separation in unstable thin liquid films

Rajesh Khanna,* Narendra Kumar Agnihotri,† and Manish Vashishtha‡
Department of Chemical Engineering, Indian Institute of Technology Delhi, New Delhi 110016, India

Ashutosh Sharma§
Department of Chemical Engineering, Indian Institute of Technology Kanpur, Kanpur 208016, India

Prabhat K. Jaiswal‖ and Sanjay Puri¶
School of Physical Sciences, Jawaharlal Nehru University, New Delhi 110067, India

(Received 14 January 2010; revised manuscript received 4 May 2010; published 2 July 2010)

We study universality in the kinetics of spinodal phase separation in unstable thin liquid films, via simulations of the thin film equation. It is shown that, in addition to morphology and free energy, the number density of local maxima in the film profile can also be used to identify the early, late, and intermediate stages of spinodal phase separation. A universal curve between the number density of local maxima and rescaled time describes the kinetics of the early stage in $d=2$ and 3. The Lifshitz-Slyozov exponent of $-1/3$ describes the kinetics of the late stage in $d=2$ even in the absence of coexisting equilibrium phases.

DOI: 10.1103/PhysRevE.82.011601 PACS number(s): 68.15.+e, 64.75.St, 68.18.−g

I. INTRODUCTION

The kinetics of spontaneous phase separation, usually referred to as *spinodal decomposition*, is of interest in far-from-equilibrium systems in diverse areas ranging from materials science and biological physics to cosmology and astrophysics [1]. Spinodal phase separation is characterized by a combination of early, intermediate and late stages. The early stage is marked by amplification/relaxation of initial fluctuations and dominance of the fastest amplifying mode which emerges as the spinodal wave. Further amplification and saturation of the spinodal wave leads to emergence of new phases and begins the late stage of phase separation. Domains of different phases grow as larger domains feed on smaller domains via diffusion or advection. The intermediate stage features a mix of formation of new domains as well as growth of existing domains. The dynamics of the late stage is well understood, and has been successfully explained by Lifshitz-Slyozov (LS) theory [2] and its variants. In contrast, the dynamics of the early and intermediate stages remains poorly understood. For example, it is not easy to study the time dependence of the domain size as given by correlation functions or structure factors, in the absence of well-defined phases. Experimental access to these stages suffers from the added difficulty of detecting low-amplitude and multimodal fluctuations. The present paper investigates the early and intermediate stages of spinodal phase separation in the technologically and scientifically important system of supported unstable thin liquid films [3]. Our study is based on simulations of a model thin film equation [4]. We discuss the unique universal features of these stages and present a useful marker to track their kinetics. The LS growth scenario for the thin film system is also validated for the late stage. Interestingly, many different growth laws have been reported for the late stage [5–8]. The similarity between the thin film equation and the Cahn-Hilliard (CH) equation [9] indicates that these unique features are likely to be shared by other spinodally phase-separating systems.

As in all spinodal processes, random fluctuations in the free surface of initially flat, supported thin liquid films (<100 nm) grow and evolve into two distinct phases (viz., a low-curvature and thinner flat film phase and a thicker high-curvature droplet phase) whenever ΔG shows a minimum and the spinodal parameter, $\partial^2 \Delta G/\partial h^2|_{h=h_0} < 0$ (Fig. 1). Here, ΔG is the excess intermolecular free energy (per unit area), h is the film thickness, and h_0 is the mean thickness [10,11]. Notice that the double-tangent construction for ΔG in Fig. 1 shows that the film phase-separates into phases with

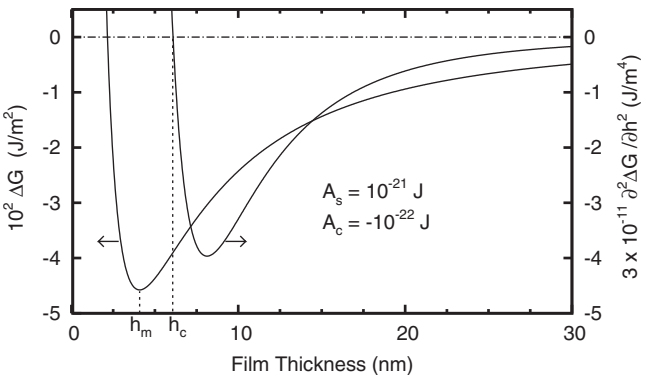

FIG. 1. Variation of the free energy per unit area (ΔG) and spinodal parameter ($\partial^2 \Delta G/\partial h^2$) with film thickness ($h$). $R=-0.1$ and δ is 5 nm. The thickness of the equilibrium flat film phase is given by h_m. Films of mean film thickness greater than h_c are spinodally unstable. Even though thinner films with $h_c > h > h_m$ are spinodally stable, they can be made unstable through nucleation.

*rajesh@chemical.iitd.ac.in
†agnik@gmail.com
‡mvche74@gmail.com
§ashutos@iitk.ac.in
‖prabhat.jnu@gmail.com
¶puri@mail.jnu.ac.in

$h=h_m$ and $h=\infty$. This should be contrasted with the usual phase-separation problems such as segregation of binary mixtures which are described by a double-well potential, i.e., there are two possible values for the equilibrium composition [12]. Actually, the droplet phase remains bounded due to overall volume conservation and so does the maximum thickness. One way to address this is to treat the droplet phase as a *defect* with changing thickness rather than a *true equilibrium phase*.

II. MODEL AND SIMULATION

We study the thin film equation which models the spatiotemporal evolution of the film's surface in supported thin liquid films. This is derived by considering a thickness-dependent excess intermolecular energy $\Delta G(h)$, and simplifying the equations of motion under the *lubrication approximation* [4]. The resulting equation can be written as a *CH* equation with a thickness-dependent effective mobility [9], $M(h)=h^3/(3\mu)$ (corresponding to Stokes flow with no slip). The total free energy is $F_s[h]=\int[\Delta G(h)+\gamma(\vec{\nabla}h)^2/2]d\vec{x}\equiv F_e+F_i$ where, F_e denotes the net excess free energy and F_i denotes the interfacial free energy. In the above expressions, γ and μ refer to surface tension and viscosity of the liquid film, respectively. The corresponding CH equation is

$$\frac{\partial}{\partial t}h(\vec{x},t)=\vec{\nabla}\cdot\left[M\vec{\nabla}\left(\frac{\delta F_s}{\delta h}\right)\right]=\vec{\nabla}\cdot\left[\frac{h^3}{3\mu}\vec{\nabla}\left(\frac{\partial\Delta G}{\partial h}-\gamma\nabla^2 h\right)\right], \tag{1}$$

where all gradients are taken in the plane of the substrate. Simulations were done for a variety of forms of $\Delta G(h)$ to uncover universal features of the early stage, if they exist. Here, a long-range van der Waals attraction due to the substrate, and a comparatively short-range van der Waals repulsion provided by a nanocoating on the substrate [13], is chosen to illustrate the results. The corresponding ΔG is shown in Fig. 1, and has the form $\Delta G=-A_c/12\pi h^2-A_s/12\pi(h+\delta)^2$. Here, A_s and $A_c(=RA_s)$ are the effective Hamaker constants for the system, which consists of the fluid bounding the film from the top, film fluid and a solid substrate (s) or coating material (c). We have taken $A_s>0$ and $A_c<0$ to represent attraction due to substrate and repulsion due to nanocoating, respectively. The thickness of the nanocoating is δ. Mean film thicknesses falling in the spinodally unstable regime, given by $\partial^2\Delta G/\partial h^2|_{h=h_0}<0$, are also shown in Fig. 1. It is seen that films of mean thickness greater than a critical film thickness h_c, where $\partial^2\Delta G/\partial h^2|_{h=h_c}=0$, will be spinodally unstable for the chosen form of ΔG.

Equation (1) is solved in the following nondimensional form to reduce parameters:

$$\frac{\partial H}{\partial T}=\vec{\nabla}\cdot\left[H^3\vec{\nabla}\left(\frac{2\pi h_0^2}{|A_s|}\frac{\partial\Delta G}{\partial H}-\nabla^2 H\right)\right]. \tag{2}$$

Here, H is the nondimensional local film thickness scaled with the mean thickness h_0; the coordinates along the substrate are scaled with the characteristic length-scale for the van der Waals case $(2\pi\gamma/|A_s|)^{1/2}h_0^2$; and nondimensional time T is scaled with $(12\pi^2\mu\gamma h_0^5/A_s^2)$. The excess energy term is completely nondimensionalized as

$$\frac{2\pi h_0^2}{|A_s|}\frac{\partial\Delta G}{\partial H}=\frac{1}{3}\left[\frac{1-R}{(H+D)^3}+\frac{R}{H^3}\right], \tag{3}$$

where $D=\delta/h_0$ is the nondimensional coating thickness. The linear stability analysis of Eq. (2) predicts a dominant spinodal wave of wavelength, L_M, given by the following expression:

$$L_M=4\pi/\sqrt{-\left.\frac{2\pi h_0^2}{|A_s|}\frac{\partial^2\Delta G}{\partial H^2}\right|_{H=1}}. \tag{4}$$

We numerically solve Eq. (2) in $d=2$ and 3 starting with an initial small-amplitude ($\simeq 0.01$) random perturbation about the mean film thickness $H=1$. In $d=2$, the system size is nL_M (n ranges from 16 to several thousands). The system size is taken to be $16L_M^2$ and $32L_M^2$ in $d=3$. Periodic boundary conditions are applied at the lateral ends. A 64-point grid per L_M was found to be sufficient when central differencing in space with half-node interpolation was combined with *Gear's algorithm* for time marching, which is especially suitable for stiff equations. The parameters D and R were chosen so that the film is spinodally unstable at $H=1$. An increase in D represents a corresponding decrease in the dimensional film thickness (h_0) for a fixed coating thickness (δ).

III. RESULTS AND DISCUSSION

A morphology-based classification of phase separation is shown in Fig. 2. Curved-droplet defects and the flat-film phase can be clearly seen in the late stage (middle frame). They are absent in the early stage (top frame), where the film surface is characterized by a fluctuating wave of increasing wavelength, a result of relaxation of stable modes and growing dominance of the spinodal wave. The intermediate stage (bottom frame) shows a mix of developing and fully developed defects. The effect of the spinodal wave can be clearly seen in the equispaced location and number of defects (~ 10 defects in $10L_M$). We now introduce the morphological feature of hills (local maxima in film profiles) to have a consistent description of the kinetics for all the three stages. The droplet phase or defect can also be considered as a hill which is surrounded by equilibrium flat film phase. Thus, all defects can be considered as hills while the converse is not true. Once each hill gets surrounded by the equilibrium flat film (as in the middle frame of Fig. 2 which shows the late stage) thereafter the term "hills" and "defects" can be used interchangeably. It can be seen that there are only hills and no defects in the top frame of Fig. 2 which shows the early stage. The bottom frame of the figure which shows the intermediate stage shows some hills which are not defects. Thus, a detailed morphological analysis of the film profile which identifies hills and defects can be used to demarcate the three stages of phase separation.

Figure 3 shows the decrease in number of hills with time. It shows three distinct stages: an early stage with exponent $-1/4$, a late LS stage with exponent $-1/3$, and an intermediate stage. These stages coincide with those found by track-

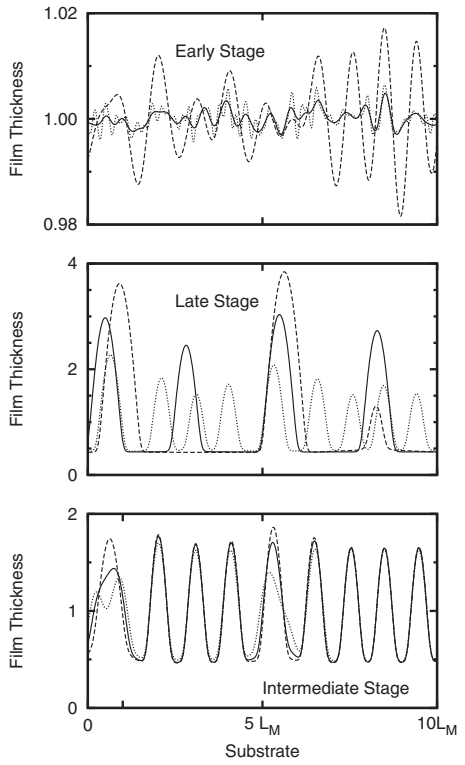

FIG. 2. Early, late, and intermediate stages of phase separation in a supported thin film. The dotted, solid, and dashed lines refer to nondimensional times 0.6, 15, and 760 (top), 23 000, 200 000, and 700 000 (middle), 2310, 2550, and 2725 (bottom). The parameters are $R=-0.1$ and $D=0.5$.

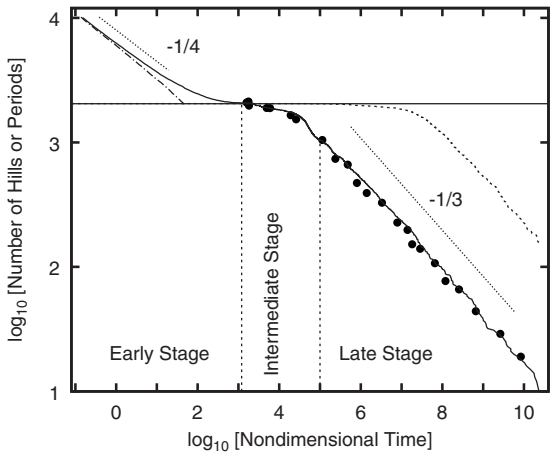

FIG. 3. Variation of the number of hills (solid line) with nondimensional time for a system size of $2048L_M$. The filled dots show the number of periods as given by the dominant wavelength from Fourier analysis of the film profile. The dash-dot line represents the results of the linearized version of Eq. (2). Dotted lines with slopes of $-1/4$ and $-1/3$ are presented to facilitate comparison with the exponents for the early and the late stage, respectively. The parameters are $R=-0.1$ and $D=0.5$. The solid horizontal line represents the number of hills corresponding to the dominant spinodal wavelength as given by linear theory result of Eq. (4). The two vertical dashed lines demarcate the early, intermediate and late stages. The dashed line on the far left shows results for nucleation in a spinodally stable film ($R=-0.1$ and $D=1$ or $h_0=5$ *nm*, see Fig. 1).

ing the morphology and validate the number of hills as a good marker of kinetics. The early stage ends when the number becomes comparable to that for the spinodal wave, shown as a horizontal line in Fig. 3. The late stage is characterized by the start of $-1/3$ slope. The limits of the intermediate stage can then be defined accordingly. An excellent matching of results with those given by dominant wavelength in the Fourier analysis of the surface morphology in the late stages (solid circles in Fig. 3) provides further support to the choice of number of hills as a marker. As expected, Fourier analysis fails to provide any characteristic length-scale in the early stages. Experimental results for all stages can be consistently described by pooling early-stage data based on number of hills, and late-stage data based on Fourier analysis. In particular, Fourier analysis allows access to detailed morphological features through quantities like the structure factor and correlation function, probability distribution of domain sizes etc.

The $-1/3$ exponent arises from LS theory for purely diffusive growth of domains. Essentially, $dL/dt \sim L^{-2}$ where $L(t)$ is the characteristic length scale and number of defects $\sim L^{-1}$. Notice that convection-assisted dynamics, whereby defects are subjected to bulk movement also, yields a slightly different exponent of $\sim -2/5$ in simulations [8]. The exponent is also different from ~ -0.44 as seen in Sung *et al.*'s experiments on phase separation of thin films of polymer blends [5]. It is likely that their experimental conditions lie somewhere between $d=2$ and 3. They attempted a crossover to $d=2$ from $d=3$ by taking progressively thinner films. Maybe the crossover was not achieved fully in those experiments. The $-1/4$ exponent arises in linear theory from the elimination of stable wavelengths in the initial fluctuations. The relevant decay for wave vector k is obtained from the dispersion relation as $\partial h(k,t)/\partial t \sim \exp(-k^4 t)$. The dashed-dotted line in Fig. 3 presents the results for the linearized version of Eq. (2).

There has been confusion about the distinction between the nucleation and spinodal processes in thin films. To address this we have also undertaken simulation of growth in spinodally stable films. We emphasize that the differences arise primarily in the early stages with nucleation being characterized by a typical onset time. However, the late-stage growth dynamics is universal with an exponent $-1/3$ (Fig. 3). Detailed morphological analysis may be required to differentiate between the two growth scenarios [14].

These stages can be readily identified in the evolution of the free energy also (Fig. 4). In the early stage, there is not much change in F_s, F_e, and F_i. This stage ends with a sharp increase in F_i and a corresponding decrease in F_e. In the late stage, there is a smooth decrease in both F_i and F_e. F_i depends on the sum of squares of local slopes. The random perturbations at the start result in a high value of the interfacial energy. The smoothening of these leads to a decrease in local slopes and F_i (bottom frame of Fig. 4). The subsequent emergence of the high-curvature defects and their growth lead to increase in F_i. On the other hand, F_e depends on the local thickness and decreases with reduction of thickness for films in the spinodal regime. The initial increase in the minimum thickness (inset of Fig. 5), a result of reducing ampli-

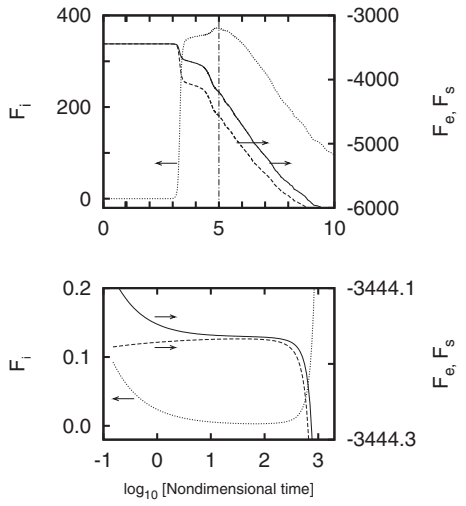

FIG. 4. Variation of the interfacial free energy (F_i, dotted curve), excess free energy (F_e, dashed curve) and total free energy (F_s, solid curve) with nondimensional time. The vertical dashed-dotted line in the top frame, which marks the maximum value of F_i, signifies the end of the intermediate stage and onset of the late stage of phase separation. The bottom frame shows the magnified view of the three energies in the early stage. The parameters are $R=-0.1$ and $D=0.5$.

tude of stable components of the surface perturbation, leads to a slight increase in F_e. As the minimum thickness passes through a maximum and starts decreasing (inset of Fig. 5), F_e also starts decreasing (bottom frame of Fig. 4). The total free energy decreases all the time, showing the spontaneous nature of the phase separation. Again, an analysis of the film profiles shows that the classification based on free energy is consistent with the analysis based on the number of hills as well as morphology. We remark that the number of hills do not provide a clear indication of the start and end of the intermediate stage. On the other hand, regime of increasing F_i and an exhaustive morphological analysis which covers the complete film profile can demarcate the intermediate stage well. Difficulties in experimental access to the complete morphological profile and F_i, effectively limit the utility of these markers to simulations only.

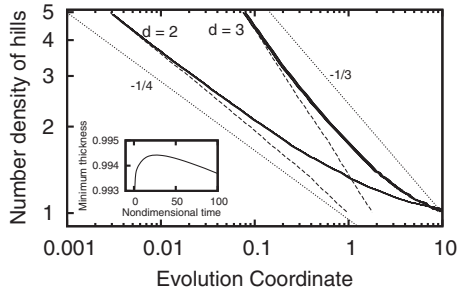

FIG. 5. Master curves in $d=2$ and 3 for variation of number density of hills with the evolution coordinate in the early stage. The dashed lines present results for the linearized version of Eq. (2) for $d=2$ and 3. We superpose data for a wide range of potential and parameters, as described in the text. Dotted lines with slopes $-1/4$ and $-1/3$ are shown to facilitate comparison with early stage exponents for $d=2$ and 3, respectively. The inset shows the variation of minimum thickness with T which is used in defining the evolution coordinate.

We obtained results for the early stage for several R ($=-0.01$, -0.1, -1.0, and -10.0) values. The D values were so chosen as to span the complete range of spinodally unstable mean film thicknesses for a given value of R. These ranges are [0.25, 2.17] for $R=-0.01$, [0.20, 0.80] for $R=-0.1$, [0.04, 0.19] for $R=-1.0$, and [0.004, 0.0239] for $R=-10.0$. Further, the system size was varied from $16L_M$ to $8192L_M$ for each R and D pair. Simulations were also carried out for other force fields, including an uncoated substrate ($D=0$) and a combination of van der Waals and polar interactions [13]. All results showed the same feature of steady decrease in number of hills (with exponent $\sim -1/4$, similar to Fig. 3), with results separated only in time scales (results not shown). The effect of system size is easily removed by plotting the number density of hills (number of hills per L_M) vs T rather than number of hills. One finds that the kinetics is independent of the system size (results not shown). This independence is especially useful for experimentalists who need not worry about the lateral size of the sample.

A master curve to describe the results for all the parameter values listed above will strongly indicate a universal early-stage kinetics. How does one rescale the results to arrive at the master curve? It is known that initial fluctuations greatly influence the kinetics for film thicknesses at the edge of the spinodal regime or in the *defect sensitive spinodal region* (DSSR), as opposed to thicknesses in the *deep inside spinodal region* (DISR) [15]. A new evolution coordinate found by dividing T by a time, T_i, at which different films are at a given morphological event during their evolution, will account for the different initial fluctuations. There can be many such choices of events, with the emergence of the flat-film phase being the most obvious one. However, the increasing dominance of the repulsive force field slows down the dynamics near this event, leading to uncertainty in estimating the corresponding times. Another event, which provides a much sharper estimate, is found by tracking the minimum thickness of the evolving film: T_i can be chosen as the time at which it reaches its largest value (see inset of Fig. 5). Indeed all results, when plotted using this evolution coordinate, collapse on a master curve as shown in Fig. 5. This shows that the early stages of phase separation in thin liquid films, as marked by the number density of hills, can be represented by a universal curve with exponent $-1/4$. Further confirmation of this universality is provided by results for the $d=3$ version of Eq. (2). They also show the same universality but with an exponent closer to $-1/3$ which matches well with the $d=3$ dynamics in experiments of Sung *et al.* (Fig. 3a of [5]). The early formation and coalescence of domains is known to have a dependence on dimensionality [1].

IV. CONCLUSIONS

In summary, we conclude that the number density of local maxima and not the usual measures like structure factors and correlation functions can be used to identify the early, late and intermediate stages of spinodal phase separation in thin films. The kinetics of the early stages for a wide range of

potentials and parameters can be described by a universal curve between the number density of hills and a rescaled time in $d=2$ and 3. This process has strong similarities with the usual phase-separation processes except for the absence of coexisting phases. Still, LS exponent of $-1/3$ governs the late stages of domain growth. Our results in this paper will facilitate the understanding of many experimental results for phase separation in thin films. We also hope that our predictions of universality in early-stage dynamics will be put to experimental test.

ACKNOWLEDGMENT

R.K. acknowledges the financial support of Department of Science and Technology, India.

[1] *Kinetics of Phase Transitions*, edited by S. Puri and V. K. Wadhawan (CRC, Boca Raton, FL, 2009).
[2] I. M. Lifshitz and V. V. Slyozov, J. Phys. Chem. Solids **19**, 35 (1961).
[3] R. V. Craster and O. K. Matar, Rev. Mod. Phys. **81**, 1131 (2009).
[4] E. Ruckenstein and R. K. Jain, J. Chem. Soc., Faraday Trans. **70**, 132 (1974).
[5] L. Sung, A. Karim, J. F. Douglas, and C. C. Han, Phys. Rev. Lett. **76**, 4368 (1996).
[6] R. Xie, A. Karim, J. F. Douglas, C. C. Han, and R. A. Weiss, Phys. Rev. Lett. **81**, 1251 (1998).
[7] R. Limary and P. F. Green, Langmuir **19**, 2419 (2003).
[8] K. B. Glasner and T. P. Witelski, Physica D **209**, 80 (2005).
[9] V. S. Mitlin, J. Colloid Interface Sci. **156**, 491 (1993).
[10] A. Sharma and A. T. Jameel, J. Colloid Interface Sci. **161**, 190 (1993).
[11] A. Sharma and R. Khanna, Phys. Rev. Lett. **81**, 3463 (1998).
[12] A. J. Bray, Adv. Phys. **43**, 357 (1994).
[13] R. Khanna, A. T. Jameel, and A. Sharma, Ind. Eng. Chem. Res. **35**, 3081 (1996).
[14] R. Seemann, S. Herminghaus, and K. Jacobs, Phys. Rev. Lett. **86**, 5534 (2001).
[15] R. Verma and A. Sharma, Ind. Eng. Chem. Res. **46**, 3108 (2007).